

# Advanced Intrinsic Correction of System Delays for Radial Trajectories

Martin Krämer<sup>1</sup> and Jürgen R Reichenbach<sup>1</sup>

<sup>1</sup>Medical Physics Group, Institute of Diagnostic and Interventional Radiology, Jena University Hospital - Friedrich Schiller University Jena, Jena, Germany

**Target Audience** – Researchers interested in the correction of radial trajectory errors caused by axis dependent system delays.

**Purpose** – With recent advances in computation and image processing capabilities non-Cartesian acquisition techniques using radial trajectories are increasingly used for a multitude of MR imaging applications. These techniques, however, are very sensitive against imperfections of the gradient and sampling hardware of the MR system that result in discrepancies between the expected and the actual  $k$ -space scanning trajectory<sup>1</sup>. For the majority of MR scanners, the system's specific delays can be separated into an orientation dependent part, which varies with the actually active physical gradient axis, and a major contribution, which is constant on all gradient axes. We have recently presented an algorithm which is able to correct for the axis independent contributions by performing a computational low cost per-scan calibration without the need to acquire any additional calibration data<sup>2</sup>. In this work we extend the algorithm to also correct for the remaining axis dependent contributions by iteratively minimizing a calibration function.

**Methods** – The new improved algorithm starts by first performing the initial correction of axis independent delays in radial direction as previously described<sup>2</sup> (Fig. 1, Part I). Briefly, a modulation of the radial input data is performed by shifting all readouts equally along the readout direction in  $N$  discretized  $k$ -space steps  $\Delta k_r$ . For each  $\Delta k_r$  2D gridding<sup>3</sup> is performed followed by an inverse 2D-FFT, resulting in  $N$  images  $I_{\Delta k_r}(x, y)$ . By calculating the sum of the magnitude of all image voxels a calibration function is obtained which is analyzed for the first maximum closest to  $\Delta k_r = 0$

$$f(\Delta k_r) = \sum_{x,y} |I_{\Delta k_r}(x, y)|$$

to obtain  $\Delta k_{r-opt}$ , which represents the best possible correction of axis independent delays. To correct for the remaining gradient axis dependent system delays a modulation of the radial data is necessary in the in-plane  $x$  and  $y$  directions by taking the radial rotation angle of each readout into account including the sinus and cosine projections of the delays  $\Delta k_x$  and  $\Delta k_y$  acting in  $x$ - and  $y$ -direction<sup>1</sup>, respectively. Using the previous algorithm for this purpose would, however, be computationally highly inefficient since a 2D modulation is required. The algorithm thus uses an iterative Nelder-Mead Simplex method (Fig. 1 Part II) as implemented by MATLAB<sup>4</sup> to minimize

$$f(\Delta k_{r-opt}) - f_{xy}(\Delta k_x, \Delta k_y),$$

with  $f_{xy}(\Delta k_x, \Delta k_y)$  being the two-dimensional calibration function of the image  $I_{\Delta k_{xy}}(x, y)$  reconstructed by applying the axis dependent delays  $\Delta k_x$  and  $\Delta k_y$ :

$$f_{xy}(\Delta k_x, \Delta k_y) = \sum_{x,y} |I_{\Delta k_{xy}}(x, y) \cdot M(x, y)|.$$

To exclude noise contributions to the calibration function, e.g., caused by gridding side lobes and aliasing artifacts outside of the object, the reconstructed images are multiplied with a binary mask  $M(x, y)$  of the image  $I_{\Delta k_{r-opt}}(x, y)$  obtained from the initial correction of the axis dependent delays. Start values for the iterative calculation of the axis dependent delays are also supplied by the result of the initial algorithm (Part I). To reduce computation time the complete analysis is only performed on a subset of the radial input data, e.g., central slice and first repetition if applicable. Application of axis dependent delays  $\Delta k_x$  and  $\Delta k_y$  for reconstruction of  $I_{\Delta k_{xy}}(x, y)$  is performed during 2D gridding by shifting the radial  $k$ -space coordinates of all individual readouts correspondingly.

To validate the algorithm phantom and *in vivo* experiments were performed on a clinical 3T system (Siemens Trio). A 360° radial sequence with parameters 240 x 240 acquisition matrix, 220 x 220 mm<sup>2</sup> field of view (FOV), 706 Hz/pixel acquisition bandwidth, 85 ms repetition time (TR) and 3.7 ms echo time (TE) was used for the phantom measurements, whereas the *in vivo* cardiac measurements were performed using a golden-angle<sup>5,6</sup> radial sequence with parameters 144 x 144 acquisition matrix, 245 x 245 mm<sup>2</sup> FOV, 489 Hz/pixel acquisition bandwidth, 2.7 ms TR and 1.5 ms TE.

**Results** – Calculated discrete maps of  $f_{xy}(\Delta k_x, \Delta k_y)$  demonstrate that the iterative algorithm successfully estimates the minimum of the calibration function (for details see Fig. 2), yielding the axis delays  $\Delta k_x$  and  $\Delta k_y$ . The estimated axis delay differences  $\Delta k_x - \Delta k_y$  were in line with separate phantom calibration measurements<sup>1</sup>. Reconstructed images, however, show only small, marginal improvements compared to correcting axis independent delays only (Fig. 3). Nevertheless, image quality is improved by the correction of axis dependent delays in areas towards the FOV edges.

**Discussion** – For the used clinical MR system only small improvements in image quality were achieved by correcting axis dependent delays with radial imaging. The delays, however, were properly estimated by the proposed algorithm – enabling a per scan calibration based on raw measurement data which also works for *in vivo* data. Improvements in image quality are expected to be more pronounced on MR systems with larger axis delays (e.g. pre-clinical systems or clinical systems with insufficient delay pre-compensation). The results also suggest that with the used MR system a correction of axis delays appears not mandatory if axis independent delays are already corrected.

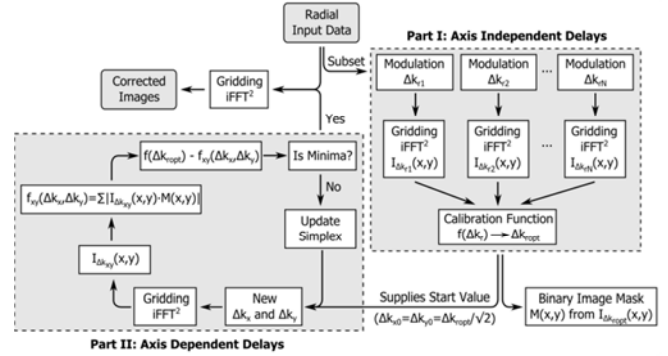


Fig. 1: Scheme of the new delay estimation algorithm consisting of two parts. Values from the fast estimation of axis independent delays<sup>2</sup> (Part I) are used as start values for the iterative estimation of axis dependent delays (Part II). The algorithm is described in detail in the methods section.

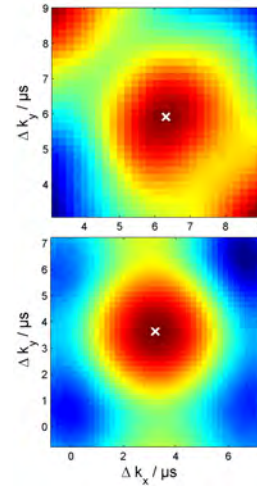


Fig. 2: Maps of  $f_{xy}(\Delta k_x, \Delta k_y)$  calculated for discrete points of  $\Delta k_x$  and  $\Delta k_y$  around  $\Delta k_{r-opt} = 6.2 \mu s$  for the phantom (top) and  $3.3 \mu s$  for the *in vivo* cardiac data (bottom). The  $k$ -space shifts  $\Delta k$  are given here in  $\mu s$ , i.e. timing delays, by using the relationship:

$$\Delta k[\mu s] = \Delta k \left[ \frac{1}{mm} \right] \cdot FOV \cdot d_t$$

with  $d_t$  being the dwell time (in  $\mu s$ ). The points marked by the white cross ( $\times$ ) are the result of the iterative estimation of  $\Delta k_x$  and  $\Delta k_y$  with the proposed algorithm. The detected axis delays were  $\Delta k_x = 5.9 \mu s$  and  $\Delta k_y = 6.3 \mu s$  for the phantom and  $\Delta k_x = 3.6 \mu s$  and  $\Delta k_y = 3.2 \mu s$  for the cardiac measurement.

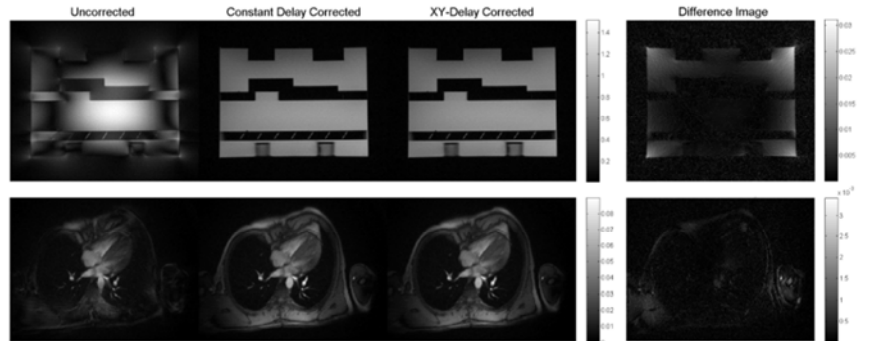


Fig. 3: Reconstructed images without delay correction, with previous correction of only constant, axis independent delays and full correction of gradient delays. The absolute difference images show the difference between the correction with axis independent delays only and the new improved algorithm that also corrects for axis dependent delays.

**References** – [1] Peters DC, et al. Magn Reson Med, 2003 [2] Biermann J, et al., ISMRM 2014, #1445 [3] Zwart NR, et al. Magn Reson Med, 2012 [4] Lagarias JC, et al. SIAM J Optim 1998. [5] Winkelmann S, et al., IEEE Trans Med Imaging, 2007 [6] Krämer M, et al., J Magn Reson Imaging, 2014